Direct-Coupled-Resonator Filters*

SEYMOUR B. COHN†, SENIOR MEMBER, IRE

Summary—A new analysis is given of direct-coupled-resonator filters that results in excellent response at much greater bandwidths than has previously been possible. The method relies on the fact that the coupling elements can be made into perfect impedance inverters, or "quarter-wave" transformers, by the addition of negative elements in lumped-constant circuits, or of short negative lengths of line in waveguide and transmission-line circuits. Specific design formulas are given for filters constructed of lumped-constant elements, waveguide, and strip or other TEM transmission line, and for pass band response functions of the maximally flat and Tchebycheff types. The formulas include a simple frequency transformation that corrects for the frequency sensitivity of the coupling reactances, and thereby greatly improves the design accuracy for both lumped-constant and microwave types when the bandwidth is more than a few per cent. Exact response curves computed from typical filter designs are compared to the prototype-function response curves, and it is shown that the design formulas give good results with bandwidths of at least 20 per cent in guide wavelength in the case of waveguide filters, or 20 per cent in frequency for TEM-mode transmission-line and lumped-constant filters.

Introduction

IN ORDER to achieve a narrow bandwidth in band-pass filters at high frequencies, it is necessary to utilize high-Q resonant circuits or cavities coupled loosely to each other in cascade. Fig. 1 shows lumped-constant, waveguide, and strip-transmission-line examples of this coupled-resonator class of filters. The relative steepness of cutoff increases with the number of resonators, and therefore methods of synthesizing filters with any number of resonators to have any desired physically realizable response are of particular interest. Considerable work has been done prior to this program on such methods, and for sufficiently narrow bandwidths adequate design formulas are available [1–11]. However, as the bandwidth is increased above 1 per cent, the accuracy of most previous design formulas deteriorates, and therefore a reexamination of the problem was considered desirable. This has been done for the case of direct coupling between resonators by utilizing a different analytical approach than has been used before, and the resulting design equations are given in an easy-to-use form in this paper. In the case of waveguide, strip-line, and other transmission-line filters of this class, a substantial improvement in design accuracy is obtained over prior results, and precise designs are now possible for bandwidths of at least 20 per cent in guide wavelength in the case of waveguide filters, or 20 per cent in frequency for the TEM-mode transmission-line filters. The design equations for the lumped-constant circuits of Fig. 1 are included for completeness, and because they are in a form particularly convenient for design application. In addition, the formulas include a simple frequency transformation that corrects for the frequency sensitivity of the coupling reactances (which have been previously assumed to be constant), and thereby greatly improves the design accuracy for both lumped-constant and microwave types when the bandwidth is more than a few per cent.

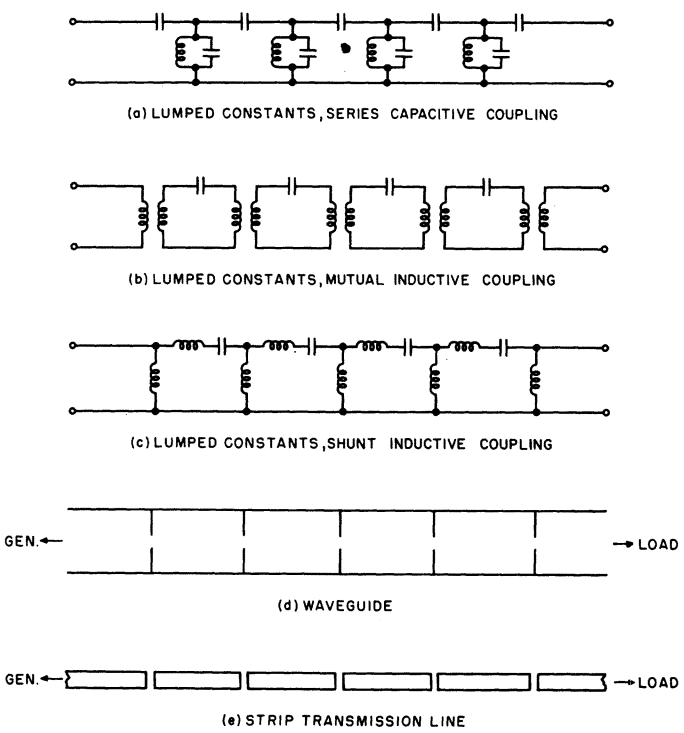

Fig. 1—Direct-coupled-resonator filters of various constructions.

The work described in this paper on direct-coupled-resonator filters began originally as a survey of design methods for narrow-band waveguide filters. Such filters have been constructed in two ways. In one, waveguide cavities are formed by inductive irises spaced approximately a half-wavelength apart, the individual cavities being coupled to each other through quarter-wavelength waveguide transformers. In the other, adjacent cavities are coupled directly to each other by single irises. The quarter-wave-coupled type permits tuning of the individual cavities before assembly, and the iris dimensions are relatively noncritical. On the other hand, the direct-coupled type is much more compact, has fewer parts, and is capable of successful operation over a greater bandwidth. Recent advances in alignment procedures [5] and iris design have largely eliminated the disadvantages of direct-coupled-cavity filters, and therefore it is believed that their use will predominate in the future.

* Original manuscript received by the IRE, June 22, 1956; revised manuscript received, October 15, 1956. The work described in this paper was supported by the Signal Corps under Contract No. DA 36-039SC-63232.

† Stanford Res. Inst., Menlo Park, Calif.

In the case of quarter-wave-coupled waveguide-cavity filters, Mumford's design method is a convenient one and sufficiently accurate for bandwidths up to a few per cent [2]. His formulas are based on a lumped-constant filter prototype having the maximally flat response, but they may be extended easily to apply to other responses, such as the Tchebycheff equal-ripple response. However, a study of the literature on direct-coupled waveguide filters has revealed three published design methods [3, 8, 9], each of which gives different results from the others. In order to evaluate these methods, and to determine the extent of the approximations involved, a fourth approach mentioned above has been used. The result is a still different set of design relationships. This new analysis is given in this paper and its accuracy is compared with the other three. For extremely narrow bandwidths, all of the methods are good, but for bandwidths exceeding approximately 1 per cent the new method is the most precise, and it may be applied successfully to far greater bandwidths.

The analysis in this paper relies on the fact that the coupling elements can be made into perfect impedance inverters, or "quarter-wave" transformers, by the addition of negative elements in lumped-constant circuits, or of short negative lengths of line in waveguide and transmission-line circuits. These elements or line lengths may then be absorbed into the resonators. In this manner an exact design is achieved in the neighborhood of resonance. Because the "quarter-wave" quality of the impedance inverters is a broad-band one, good accuracy is maintained over a wide range. However, the variation of the coupling reactances, or susceptances, with frequency causes the response of the filter to be unsymmetrical, although a close approximation of this effect may be taken into account by means of the frequency-transformation formulas given in this paper.

Design Formulas

Low-Pass Prototype

The design formulas for the various types of direct-coupled-resonator filters considered in this paper are based on the low-pass filter prototype shown in Fig. 2. General formulas are given in the figure for the element values that will yield either the maximally flat or the Tchebycheff (equal ripple) insertion-loss response [12, 13]. For convenience, the following conditions are assumed: 1) the pass band edge occurs at $\omega' = 1$ (*i.e.*, at $f' = 1/2\pi$), 2) the left-hand load resistance is one ohm, and 3) the first element, g_1 is a shunt capacitance. Thus the elements of odd order $g_1, g_3, g_5, \cdots$, are shunt capacitances, and their values given by the formulas are in farads, while the elements of even order $g_2, g_4, g_6, \cdots$, are series inductances, and are given in henries. The last element, g_n, is a shunt capacitance if n is odd, and a series inductance if n is even. Inspection of the formulas shows that the right-hand resistance, r, is one ohm for all cases considered, except that of Tchebycheff response with n even. Also, with the exception of that case, the set of element values $g_1, g_2, g_3, \cdots, g_n$ is symmetrical. All needed quantities are defined in the formulas or response curves of the figure. The insertion-loss functions are also given in Fig. 2 for both maximally flat and Tchebycheff response.

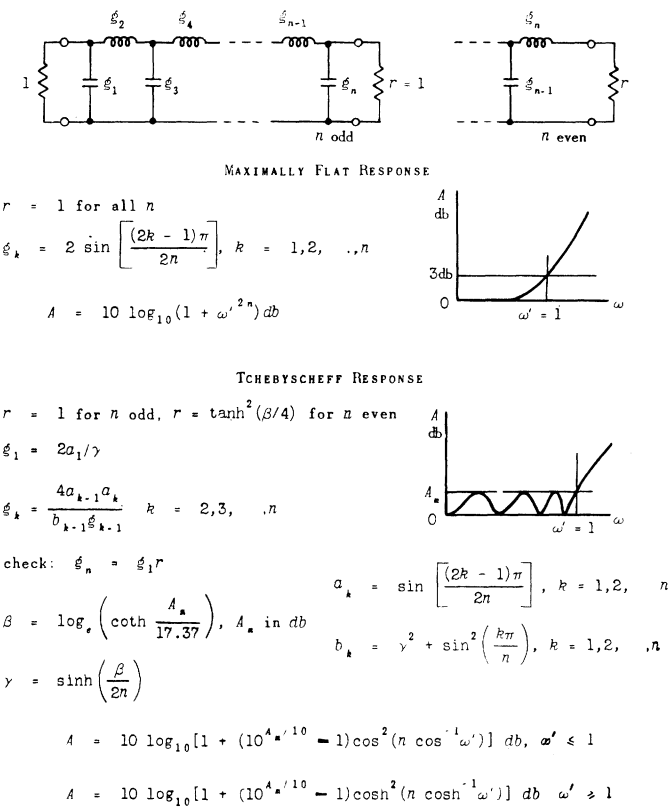

Fig. 2—Prototype low-pass filter and its design equations for maximally flat and Tchebycheff response.

Lumped-Constant Filter Formulas

Fig. 3 gives the design relationships for lumped-constant coupled-resonant-circuit filters for both capacitive and inductive coupling. The derivation of the formulas is outlined later on. The load resistances may have any value, and may be equal or unequal to each other, as desired. The resonant-circuit elements L_{rk}, C_{rk}, may be selected to have any convenient sizes as long as they are large enough that the actual inductances and capacitances in the composite filter circuit are all positive. The formulas for the individual elements utilize the values $g_1, g_2, g_3, \cdots, g_n$ of the low-pass prototype filter, which are computed from the formulas in Fig. 2 for the particular insertion-loss response desired.

The insertion-loss curves sketched in Fig. 3 show the relationships between the band-pass and prototype responses. The band-pass response is obtained from the prototype response by transforming the frequency scale such that f_0 of the band-pass filter corresponds to $f' = 0$ of the low-pass filter, and the band edges f_1 and f_2 of the band-pass filter correspond to the band edge f_1' of the prototype. In the design equations, f_1' should be set equal to $1/2\pi$ if it is desired to have the insertion loss at

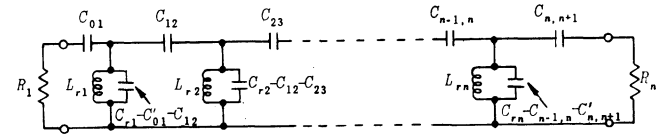

$$L_{rk}C_{rk} = \frac{1}{\omega_o^2}$$

$$C_{01} = \frac{1}{\omega_o}\left(\frac{w'C_{r1}/R_1g_1}{1 - w'C_{r1}R_1/g_1}\right)^{\frac{1}{2}}$$

$$C_{n\,n+1} = \frac{1}{\omega_o}\left(\frac{w'C_{rn}r/R_ng_n}{1 - w'C_{rn}R_n/g_n}\right)^{\frac{1}{2}}$$

$$C_{jk} = w'\left(\frac{C_{rj}C_{rk}}{g_jg_k}\right)^{\frac{1}{2}} \text{ for } C_{12} \text{ to } C_{n-1,n}$$

$$C'_{01} = \frac{C_{01}}{1 + \omega_o^2C_{01}^2R_1^2}$$

$$C'_{n,n+1} = \frac{C_{n,n+1}}{1 + \omega_o^2C_{n,n+1}^2R_n^2}$$

$g_1, g_2, \ldots, g_n$ = prototype elements in farads and henries from Fig. 2.

r = right-hand load resistance in Fig. 2.

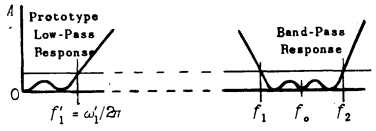

Note: The filter circuit is symmetrical if $R_1 = R_n$ and $C_{rk} = C_{r,n+1-k}$.

$$f_o = f_1 + f_2 - [(f_2 - f_1)^2 + f_1f_2]^{\frac{1}{2}}$$

$$w' = \left(\frac{f_o}{f_1} - \frac{f_o}{f_2}\right)\left(\frac{f_o}{f_1'}\right)$$

For $f_2/f_1 < 0.05$:

$$f_o \approx \sqrt{f_1f_2}$$

$$w' \approx \frac{f_2 - f_1}{f_1'}$$

(a)

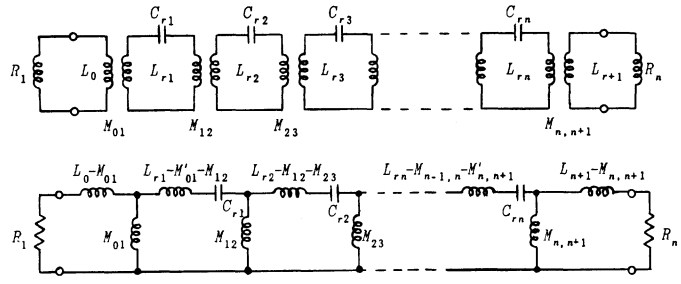

$$\omega_o^2L_{rk}C_{rk} = 1 \text{ for } k = 2 \text{ to } n-1$$

$$\omega_o^2L_{r1}C_{r1} = 1 + \frac{w'L_0}{g_1R_1},$$

$$\omega_o^2L_{rn}C_{rn} = 1 + \frac{w'L_{n+1}r}{g_nR_n}$$

$$\omega_oM_{jk} = \pm w'\sqrt{\frac{L_{rj}L_{rk}}{g_jg_k}} \text{ for } M_{12} \text{ to } M_{n-1,n}$$

$$\omega_oM_{01} = \pm\sqrt{\frac{w'(R_1^2 + \omega_o^2L_0^2)}{\omega_o^2C_{r1}g_1R_1}}$$

$$\omega_oM_{n,n+1} = \pm\sqrt{\frac{w'r(R_n^2 + \omega_o^2L_{n+1}^2)}{\omega_o^2C_{rn}g_nR_n}}$$

$g_1, g_2, \ldots, g_n$ = prototype elements in farads and henries from Fig. 2.

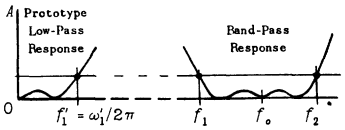

r = right-hand load resistance in Fig. 2

$$f_o = f_1 + f_2 - [(f_2 - f_1)^2 + f_1f_2]^{\frac{1}{2}}$$

$$w' = \left(\frac{f_o}{f_1} - \frac{f_o}{f_2}\right)\left(\frac{f_o}{f_1'}\right)$$

For $f_2/f_1 < 0.05$:

$$f_o \approx \sqrt{f_1f_2}$$

$$w' \approx \frac{f_2 - f_1}{f_1'}$$

(b)

Fig. 3—(a) Design formulas for capacitive-coupled lumped-constant filter. (b) Design formulas for inductive-coupled lumped-constant filter.

the pass-band edge be 3 db in the maximally flat case or be equal to the ripple level in the Tchebycheff case. However, an f_1' corresponding to any other pass band-edge insertion loss may be used if desired. The insertion-loss curves of the band-pass filter and the low-pass prototype vary in the same manner as a function of $|f-f_0|$ and f'. For narrow bandwidth, the band-pass insertion loss may be computed from the formula for the low-pass filter by replacing f'/f_1' by $2|f-f_0|/(f_2-f_1)$. For bandwidths of more than a few per cent, if one assumes that the coupling reactances do not vary with frequency, a better transformation requires that f'/f_1' be replaced by $|f/f_0-f_0/f|/(f_2/f_0-f_0/f_2)$, where f_0 is related to f_1 and f_2 by $f_0=\sqrt{f_1f_2}$. However, the coupling reactances necessarily vary with frequency, and for bandwidths of more than a few per cent a superior transformation for the filter circuits of Fig. 3 is to replace f'/f_1' by:

$$\frac{f'}{f_1'} = \left|2 - \frac{f_0}{f} - \frac{1}{2 - \frac{f_0}{f}}\right| \Bigg/ \left[2 - \frac{f_0}{f_2} - \frac{1}{2 - \frac{f_0}{f_2}}\right] \quad (1)$$

where f_0 is now related to f_1 and f_2 by

$$f_0 = f_1 + f_2 - \sqrt{(f_2 - f_1)^2 + f_1f_2}. \quad (2)$$

For constant coupling reactance, the proper formula for w' in Fig. 3 would be $w'=(f_2-f_1)/f_1'$. However, a close approximation of the effect of reactance variation with frequency is obtained when the following relationship for w' is used:

$$w' = \left(\frac{f_0}{f_1} - \frac{f_0}{f_2}\right)\frac{f_0}{f_1'}. \quad (3)$$

In order to evaluate the accuracy of the design formulas for a moderately wide bandwidth, a six-resonant-circuit lumped-constant filter was designed and its exact response computed. The result is compared to the prototype function in Fig. 4. The response was designed to be maximally flat with 3-db points ω_2 and ω_1 in the ratio 1.20:1. The agreement between the curves is seen to be very good, despite the fact that the response is highly unsymmetrical on a linear frequency scale.

Waveguide Filter Formulas

Fig. 5 gives the formulas for direct-coupled waveguide filters. The electrical lengths, ϕ_1, of the cavities and the normalized inductive reactances, $X_{i,i+1}$, of the irises are computed in terms of the prototype elements g_1, g_2, g_3, $\cdots$, and the desired guide-wavelength pass band limits λ_{g1} and λ_{g2}. As in the case of the lumped-constant filters, the formulas take into account the variation of the inductive coupling reactances with frequency. The iris reactance is assumed to vary in inverse proportion to guide wavelength (this is an excellent approximation for inductive windows or apertures in thin walls and for inductive posts [14]). If the coupling reactances were

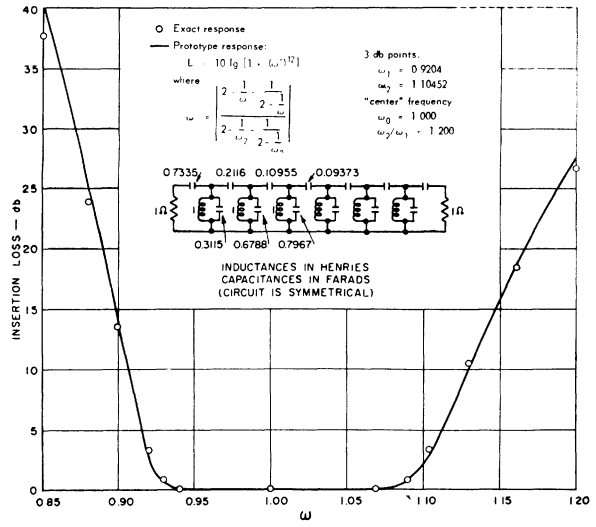

Fig. 4—Insertion loss of lumped-constant filter with six resonant circuits designed for maximally flat response.

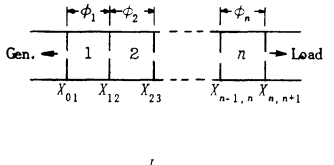

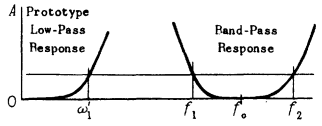

Note. $X_{i,i+1} = X_{n-i,n+1-i}$ and $\phi_i = \phi_{n+1-i}$, i.e., the structure is symmetrical

$$X_{i,i+1} = \frac{\frac{L}{\sqrt{g_i g_{i+1}}}}{1 - \frac{L^2}{g_i g_{i+1}}},$$

$$\phi_i = 180° - \frac{1}{2}\left[\tan^{-1}(2X_{i-1,i}) + \tan^{-1}(2X_{i,i+1})\right]$$

$X_{i,i+1}$ = normalized iris reactance at λ_{g0} ϕ_i = phase length at λ_{g0}

$\lambda_{g0} = \frac{1}{2}(\lambda_{g1} + \lambda_{g2})$ = center guide wavelength

$g_1, g_2, \ldots, g_n$ = prototype elements in farads and henries from Fig 2

$g_0 = L$, $g_{n+1} = \frac{L}{r}$

r = right-hand load resistance in Fig 2

$$L = \frac{\pi}{\omega_1'}\left[\frac{\lambda_{g1} - \lambda_{g2}}{\lambda_{g1} + \lambda_{g2}}\right], \quad L \approx \frac{\pi}{2\omega_1'}\left(\frac{\lambda_{g0}}{\lambda_0}\right)^2\left(\frac{f_2 - f_1}{f_0}\right) \quad \text{for} \quad \frac{f_2 - f_1}{f_0} < 0.01$$

ω_1' = pass-band edge of prototype filter

$\lambda_{g1}, \lambda_{g2}, f_1, f_2$ = corresponding pass-band edges of waveguide filter

f_0, λ_0 evaluated at λ_{g0}

Fig. 5—Formulas for inductive-iris-coupled waveguide filters.

independent of frequency, the response of the filter would be expected theoretically to be symmetrical on a $1/\lambda_g$ scale. However, the guide-wavelength dependence of the coupling reactances has the very interesting effect of making the filter response symmetrical on a λ_g scale. The predicted insertion-loss response may be computed from the formulas given in Fig. 2 for the low-pass prototype by substituting

$$\frac{\omega'}{\omega_1'} = 2\left(\frac{\lambda_{g0} - \lambda_g}{\lambda_{g1} - \lambda_{g2}}\right). \tag{4}$$

As in the lumped-constant case, ω_1' should be set equal to unity if the pass band-edge insertion loss is desired to be 3 db for maximally flat response or to be the equal-ripple level for Tchebycheff response. Otherwise, ω_1' should be given the value that corresponds to the desired edge insertion loss in the low-pass prototype function.

The formulas of Fig. 5 differ from other formulas for direct-coupled filters in a number of important respects. First, all other published design formulas are based on frequency-independent coupling reactances, which are physically unrealizable. For bandwidths of more than a few per cent, this leads to errors in the pass band limits and in the steepness of cutoff. Aside from this, Southworth's formula [8] for $X_{i,i+1}$ differs from that of Fig. 5. If the denominator $(1-L^2/g_ig_{i+1})$ of the relation for $X_{i,i+1}$ in Fig. 5 is replaced by unity, the result is equivalent to Southworth's. However, the omission of the term L^2/g_ig_{i+1} leads to appreciable error in a design for even a 1 per cent bandwidth, although for extremely narrow bandwidths the discrepancy becomes negligible. Fano and Lawson's analysis [3] has been found to contain typographical errors. When the errors are corrected, the result is the same as Southworth's, except for a minor difference in the formula for ϕ_i. Riblet's formulas [9] are in a completely different form from those of Fig. 5, and hence a direct comparison cannot be made.

Fig. 6 shows a comparison of the exact vswr of filters designed by various methods to have the same bandwidth and the same response function. Perfect agreement occurs between the maximally flat prototype function and the design of this paper for the assumed bandwidth of 3 per cent. Equally good agreement was obtained on an insertion-loss scale up to at least 50 db [Fig. 6]. Although Southworth's design deviates considerably from the prototype function at low vswr values, on an insertion-loss scale it would appear to agree much better. Riblet's design method gives its best results at low vswr's in the example of Fig. 6. At the 3-db points the bandwidth error is about 8 per cent. For greater bandwidths the error in design would increase.

The vswr and insertion loss of a six-cavity waveguide filter designed by the new method for Tchebyscheff response is shown in Fig. 7. The agreement between the exact computed response and the prototype function is excellent for the design bandwidth of 2 per cent.

The new method was also tested for moderately wide bandwidths. The results for a six-cavity filter designed for maximally flat response and bandwidth of about 20 per cent are shown in Fig. 8, and for Tchebycheff response and bandwidth of about 10 per cent in Fig. 9. In both cases the agreement is good, although minor deviations from the prototype functions are observed. The pass band vswr, which gives the most exacting test, shows the most discrepancy, but the maximum pass band vswr is very low and is certainly suitable for most practical applications. The dissymmetry of these responses caused by frequency variation of the coupling

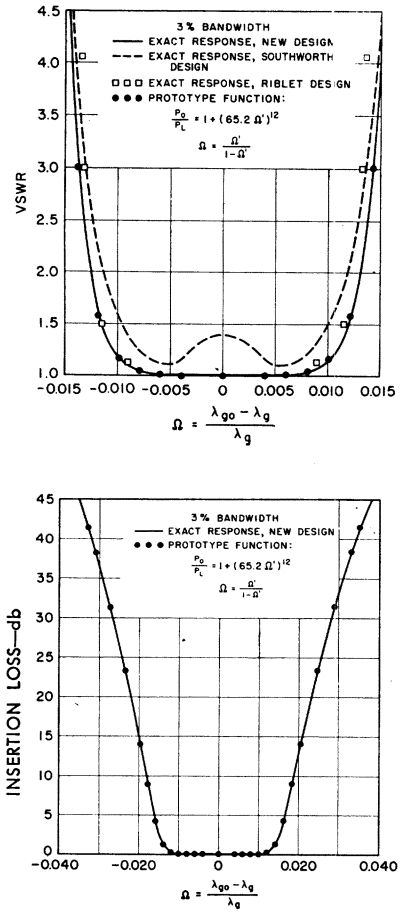

Fig. 6—VSWR and insertion loss of direct-coupled six-cavity waveguide filter designed for maximally flat response—bandwidth 3 per cent.

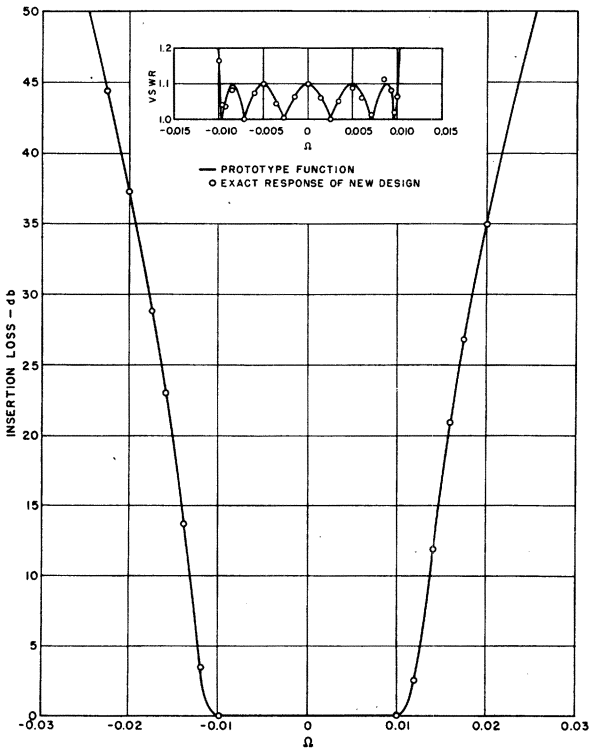

Fig. 7—Insertion loss and vswr of direct-coupled six-cavity waveguide filter designed for Tchebycheff response—bandwidth 2 per cent.

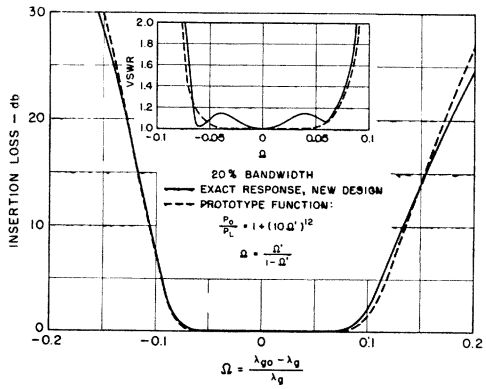

Fig. 8—Insertion loss and vswr of direct-coupled six-cavity waveguide filter designed for maximally flat response—bandwidth 20 per cent.

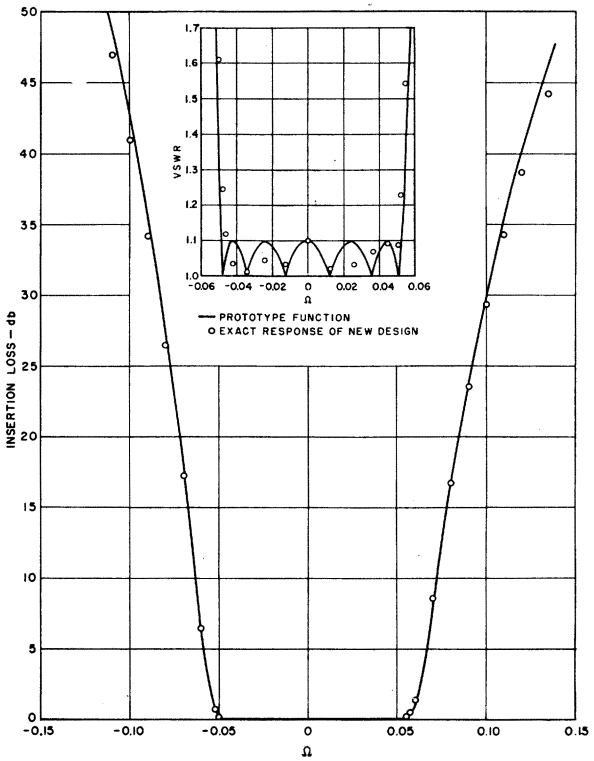

Fig. 9—Insertion loss and vswr of direct-coupled six-cavity waveguide filter designed for Tchebycheff response—bandwidth 10 per cent.

reactances is quite large, but is compensated for very well by the frequency-scale transformation that was introduced into the design formulas.

Strip-Line Filter Formulas

Strip-line direct-coupled filters can be made conveniently with either series-capacitive or shunt-inductive coupling between resonant line lengths. The formulas of Fig. 5 for waveguide filters apply in the case of inductive coupling if free-space wavelength λ is substituted everywhere for guide wavelength λ_g. The shunt inductances might consist of metal posts or strips joining the strip line to the two ground planes. However, a usually more convenient construction method uses capacitive coupling, where gaps in the strip line form the series capaci-

tances. The filter layout and design formulas are shown in Fig. 10. The filter circuit is the dual of the circuit containing inductive coupling elements, and the formulas were written directly from Fig. 5 by means of the usual duality relationships, and the substitution of free-space wavelength for guide wavelength.

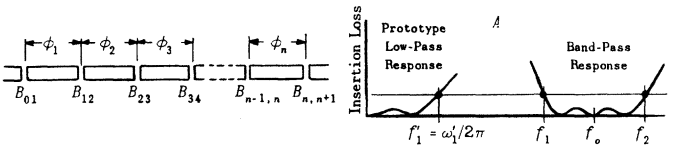

Note: $B_{i,i+1} = B_{n-i,n+1-i}$ and $\phi_i = \phi_{n+1-i}$; i.e., the structure is symmetrical.

$$B_{i,i+1} = \frac{C}{\sqrt{g_i g_{i+1}} \left(1 - \frac{C^2}{g_i g_{i+1}}\right)}$$

$$\phi_i = 180° - \frac{1}{2}\left[\tan^{-1}(2B_{i-1,i}) + \tan^{-1}(2B_{i,i+1})\right]$$

$B_{i,i+1}$ = normalized gap susceptance at f_o

ϕ_i = phase length at f_o

$$f_o = \frac{2f_1 f_2}{f_1 + f_2}$$

$g_1, g_2, \ldots, g_n$ = prototype elements in farads and henries from Fig. 2.

$g_o = C$, $g_{n+1} = \frac{C}{r}$

r = right-hand load resistance in Fig. 2.

$$C = \frac{1}{2f_1'}\left(\frac{f_2 - f_1}{f_2 + f_1}\right)$$

f_1' = pass-band edge of prototype filter

f_1, f_2 = corresponding pass-band edges of transmission-line filter

Fig. 10—Formulas for capacitive-gap-coupled transmission-line filter.

The calculation of the coupling values and line lengths in terms of the low-pass prototype elements is done the same way as for the waveguide filter. The gap dimensions to yield the required series capacitances may be obtained from experimental curves or a theoretical formula to be found in several references [10, 11, 15, 16]. If the gap is small compared to the ground-plane spacing the resonant line lengths should be measured from the center of the gap. The line-length error in this procedure is proportional to the square of the ratio of gap to ground-plane spacing, and is usually negligible. However a line length correction for the presence of the gap may be made from available formulas and data [15, 16].

The theoretical response curves of Figs. 6 to 9 apply exactly to strip-line direct-coupled filters if guide wavelength is replaced by free-space wavelength. Thus, as in the waveguide case, the response of either series-capacitive or shunt-inductive coupled strip-line filters is symmetrical on a wavelength scale rather than on a frequency scale. Therefore, to compute the insertion-loss response from that of the low-pass prototype given in Fig. 2, one should use (4) with λ replacing λ_g.

Derivation of Formulas

Basic Transformations Applicable to All Types

Fig. 11(a) shows the lumped-constant prototype and Fig. 11(b) the inverse-arm band-pass filter derived from it by the frequency transformation: $\omega' \propto (\omega/\omega_0 - \omega_0/\omega)$. In both cases the first arm is taken always to be a shunt arm. Impedance inverting transformers[1] are next inserted between the successive arms of the filter to obtain the circuit of Fig. 11(c), in which all resonant arms are series arms. The impedance-inversion property that makes this last transformation possible may be expressed simply by the well-known relationships for a quarter wavelength of transmission line: $Z_1 = K^2 Y_2$ and

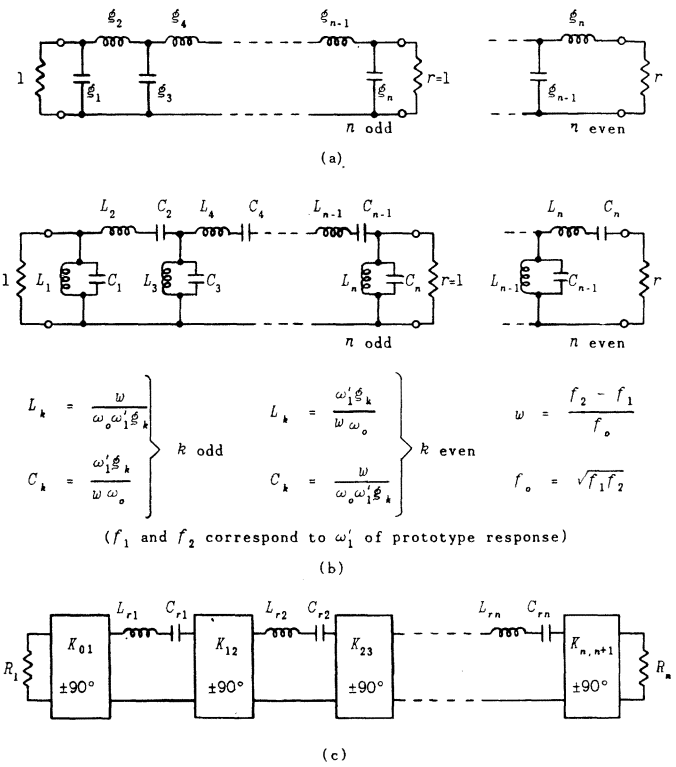

Fig. 11—Transformations from low-pass prototype to band-pass filter containing quarter-wave inverters.

$Y_1 = Z_2/K^2$, where K is the characteristic impedance (or image impedance) of the quarter-wave line (inverter), the subscript "2" denotes load impedance or admittance connected to the inverter, and the subscript "1," input impedance or admittance. Thus, for example, a shunt capacitance C viewed through the inverter appears to be a series inductance of value $L = K^2 C$, while a series inductance L appears to be a shunt capacitance of value $C = L/K^2$. The detailed steps using this concept are carried out below and lead to the desired relationships between the elements L_k, C_k in Fig. 11(b) and L_{rk}, C_{rk} in Fig. 11(c).

[1] Impedance inverters have had frequent use in network transformation. For example, see [1] and [15].

Consider the portion of the inverse-arm band-pass circuit shown in Fig. 12(a). The elements L_2 and C_2 already constitute a series arm as desired, but at an improper impedance level. This may be corrected as indicated in Fig. 12(b) by multiplying all inductances in the filter (and the load resistances) by L_{r2}/L_2, and all capacitances by L_2/L_{r2}. Next, an inversion network is introduced in Fig. 12(c) to transform the shunt arm of Fig. 12(b) into a series arm. In order for the performance of the filter to be the same in both cases, Y_3 in Fig. 12(b) and (c) must be identical. Hence it is necessary that

$$j\left(\omega C_3 - \frac{1}{\omega L_3}\right)\frac{L_2}{L_{r2}} + Y_4 = \frac{1}{K_{23}^2}\left\{j\left(\omega L_{r3} - \frac{1}{\omega C_{r3}}\right) + Z_4'\right\}.$$

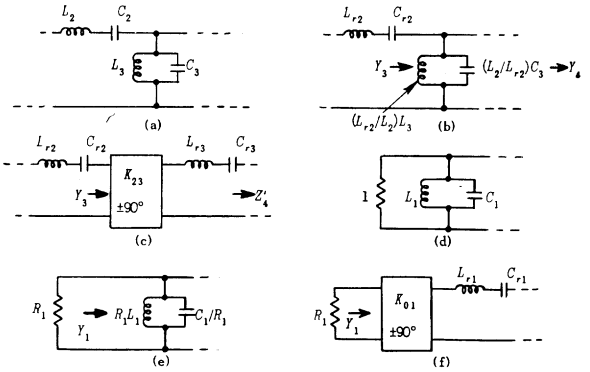

Fig. 12—Detailed transformations used in analysis.

After identifying the quantities that have the same dependence on ω, one may write

$$K_{23} = \sqrt{\frac{L_{r2}L_{r3}}{L_2C_3}}, \qquad L_{r2}C_{r2} = L_{r3}C_{r3} = \frac{1}{\omega_0^2}.$$

With the aid of the relations in Fig. 11(b), we may write, in general for arms k and $k+1$,

$$K_{k,k+1} = \frac{\omega_0 w}{\omega_1'}\sqrt{\frac{L_{rk}L_{r,k+1}}{g_k g_{k+1}}}, \qquad L_{rk}C_{rk} = \frac{1}{\omega_0^2}. \tag{5}$$

The first and last K in the filter may be computed in a similar manner. Thus, Fig. 12(d) shows the input load resistance and first shunt arm of the inverse-arm band-pass filter. In Fig. 12(e), the impedance level has been changed from one ohm to R_1 ohms. In Fig. 12(f), an inversion network is introduced to transform the shunt arm to a series arm. In order for Y_1 to be the same in Fig. 12(e) and (f), K_{01} must be chosen so that

$$K_{01} = \sqrt{\frac{L_{r1}R_1}{C_1}} = \sqrt{\frac{\omega_0 w}{\omega_1'}\cdot\frac{L_{r1}R_1}{g_1}}. \tag{6}$$

Similarly, the last inversion network is given by

$$K_{n,n+1} = \sqrt{\frac{\omega_0 w}{\omega_1'}\frac{L_{rn}R_{nr}}{g_n}} \tag{7}$$

for n odd or even.

Impedance-Inversion Networks

A number of networks that have the inversion properties of a quarter-wave transformer over a broad bandwidth are shown in Fig. 13. The characteristic impedance, K, and phase shift, β, of each network may be derived in various ways. For example, in Fig. 13(a) the short- and open-circuit input impedances of half the network are $Z_{sc} = -j/\omega C$, $Z_{oc} = j/\omega C$, and through the use of well-known relationships

$$K = \sqrt{Z_{sc}Z_{oc}} = \frac{1}{\omega C},$$

$$\beta = 2\tan^{-1}\pm\left(\frac{-Z_{sc}}{Z_{oc}}\right)^{1/2} = \pm 90°.$$

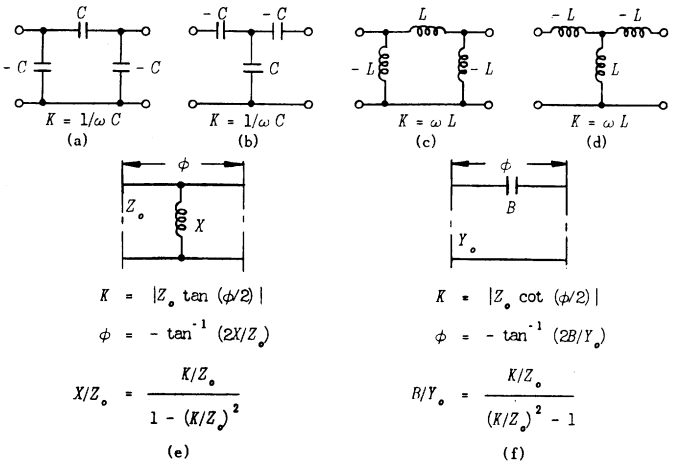

Fig. 13—Broad-band impedance-inversion networks.

For the network of Fig. 13(a) the negative sign for β is correct, but in this application the particular sign is unimportant. The important point to notice is that β is not frequency dependent, and hence the impedance-inversion property of Fig. 13(a), and also of Fig. 13(b), (c), and (d), holds at all frequencies, while the characteristic impedance has the same variation with frequency as does the kind of reactance in the network. The most suitable inversion network to choose for a given filter is one whose negative elements can be absorbed into the resonant circuits so that all element values of the composite filter are positive.

Networks in TEM transmission line and waveguide may also be devised that provide impedance inversion over very wide bandwidths. Cases utilizing a shunt inductive reactance and a series capacitive reactance appear in Fig. 13(e) and (f). For example, in the case of the

shunt inductive reactance, $X=\omega L$, negative electrical lengths of line are required on each side of the reactance. The formulas in the figure may be derived conveniently from the short- and open-circuit impedances of half the structure:

$$\beta = 2\tan^{-1} \pm \sqrt{\frac{-X_{sc}}{X_{oc}}}$$

$$= 2\tan^{-1} \pm \sqrt{\frac{-Z_0 \tan \frac{\phi}{2}}{Z_0 \tan\left\{\frac{\phi}{2} + \tan^{-1}\left(\frac{2\omega L}{Z_0}\right)\right\}}} \quad (8)$$

$$K = Z_0 \sqrt{-\tan\left(\frac{\phi}{2}\right)\tan\left[\frac{\phi}{2} + \tan^{-1}\left(\frac{2\omega L}{Z_0}\right)\right]}. \quad (9)$$

If we set $\beta = -90°$, it is necessary at ω_0 that

$$\phi = -\tan^{-1}\left(\frac{2\omega_0 L}{Z_0}\right) \quad \text{and} \quad K = Z_0 \tan\frac{\phi}{2}. \quad (10)$$

The numerator and denominator of (8) are both almost exactly proportional to ϕ, and this causes the frequency variation of β from $-90°$ to be slight enough to be neglected. Also, K is very closely proportional to ϕ.

For use in design work, a formula for $X=\omega_0 L$ in terms of K is needed. This is obtained as follows with the aid of a trigonometric identity.

$$\frac{X}{Z_0} = \frac{1}{2}\tan(-\phi) = \frac{1}{2}\tan\left(2\tan^{-1}\frac{K}{Z_0}\right)$$

$$= \frac{K/Z_0}{1-(K/Z_0)^2}. \quad (11)$$

Equivalent Circuit of a Half-Wavelength Resonator

In the case of TEM-transmission-line or waveguide direct-coupled filters, the equivalent circuit of a half-wavelength of line is required. This is given exactly in Fig. 14(b). The three reactive elements provide the frequency dependence of the circuit, while the ideal transformer provides the phase reversal of a half-wave line. Since this reversal plays no part in the filter performance, it is neglected in the approximate equivalent circuit of Fig. 14(c).

When the half-wave resonators are used in a waveguide filter, the shunt arms of Fig. 14(c) are connected almost directly in parallel with the large shunt susceptances of the inversion networks. In Fig. 14(b), it is seen that B/Y_0 is much less than unity even for moderately wide bandwidths, while the normalized susceptance of the coupling irises is much larger than unity. Hence the shunt arms may be neglected as in Fig. 14(b), where only the series-resonant arm remains. Reference to the filter schematic of Fig. 11(c) shows that the last half-wave-line equivalent may be used as the resonators, and the shunt reactance and associated negative line length of Fig. 13(e) may serve as the inversion networks. First, however, an expression for L_{r1} in terms of waveguide parameters must be obtained.

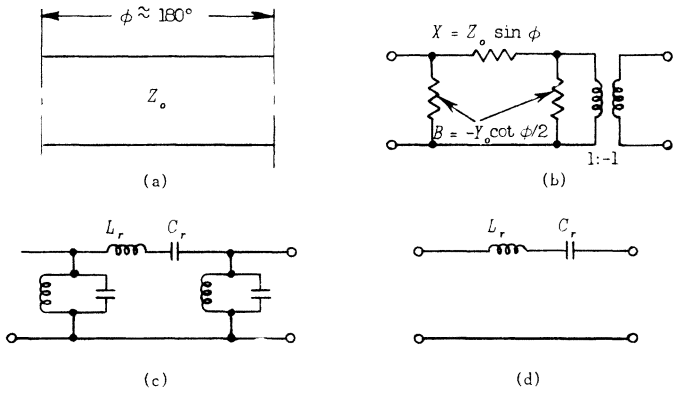

Fig. 14—Equivalent circuit of half-wavelength resonator.

Fig. 14(b) gives the reactance of the series arm as $X=Z_0 \sin\phi$. In the vicinity of $\phi=\pi$, this may be written

$$X = Z_0(\phi - \pi) = \pi Z_0\left(\frac{\lambda_{g0}}{\lambda_g} - 1\right). \quad (12)$$

In terms of the equivalent-circuit elements,

$$X = \omega L_r - \frac{1}{\omega C_r}. \quad (13)$$

A relationship between L_r and λ_g is most easily obtained by equating $dX/d\omega|_{\omega=\omega_0}$, computed from (12), to the same quantity from (13). Thus,

$$\left.\frac{dX}{d\omega}\right|_{\omega=\omega_0} = 2L_r = Z_0\left.\frac{d\phi}{d\omega}\right|_{\omega=\omega_0} \approx \pi Z_0 \frac{\lambda_{g0}/\lambda_{g2} - \lambda_{g0}/\lambda_{g1}}{\omega_2 - \omega_1}$$

and therefore

$$L_r = \frac{\pi Z_0}{2\omega_0 w}\left(\frac{\lambda_{g0}}{\lambda_{g2}} - \frac{\lambda_{g0}}{\lambda_{g1}}\right) \quad (14)$$

where $w=(\omega_2-\omega_1)/\omega_0$ and $\omega_0=(\omega_1+\omega_2)/2$. A combination of (5), (6), (7), and (14) then gives

$$\frac{K_{k,k+1}}{Z_0} = \frac{L}{\sqrt{g_k g_{k+1}}} \quad (15)$$

where, for convenience,

$$L = \frac{\pi}{2\omega_1'}\left(\frac{\lambda_{g0}}{\lambda_{g2}'} - \frac{\lambda_{g0}}{\lambda_{g1}'}\right) \quad (16)$$

$$g_0 = L, \quad g_{n+1} = \frac{L}{r}, \quad R_1 = R_n = Z_0 \tag{17}$$

$$\frac{1}{\lambda_{g0}} = \frac{1}{2}\left(\frac{1}{\lambda_{g1}'} + \frac{1}{\lambda_{g2}'}\right). \tag{18}$$

The prime marks placed on λ_{g1}' and λ_{g2}' indicate that these are the pass band limits when the inversion-network characteristic impedances $K_{k,k+1}$ are assumed to be constant with frequency. However, $K_{k,k+1}$ varies with frequency, causing the filter response to be an unsymmetrical function of λ_{g0}/λ_g, and therefore the unprimed quantities λ_{g1} and λ_{g2} will henceforth be reserved for the true pass band limits. A simple relationship between λ_g' and λ_g will now be obtained.

Frequency-Scale Correction for Waveguide Filter

The bandwidth of a multiple-resonator direct-coupled filter is dependent mainly upon the size of the internal coupling elements, and only slightly upon the input and output coupling elements. Eqs. (15) and (16) show that the relative bandwidth expressed in reciprocal guide wavelength is proportional to K/Z_0 of the internal inverting networks, while (11) shows that K/Z_0 is approximately proportional to X/Z_0. A shunt inductive iris or post in waveguide has a reactance variation very nearly proportional to λ_{g0}/λ_g. Hence, to a good approximation, $\lambda_{g0}/\lambda_g - 1 \propto K/Z_0 \propto \lambda_{g0}/\lambda_g$. For very narrow bandwidths, $\lambda_g' \to \lambda_g$, and this permits the proportionality relationship to be completed as follows:

$$\left(\frac{\lambda_{g0}}{\lambda_g}\right) - 1 = \left(\frac{\lambda_{g0}}{\lambda_g'} - 1\right)\frac{\lambda_{g0}}{\lambda_g}. \tag{19}$$

Through the use of (18) and (19), λ_{g0} is related to the pass band limits by $\lambda_{g0} = (\lambda_{g1} + \lambda_{g2})/2$. When this is substituted in (16), the formula for L given in Fig. 5 results.

Upon joining the series of half-wave lines and inversion structures, the electrical length of each resonator is 180° plus the $\phi/2$ lengths associated with the adjoining coupling reactances. With the aid of (10), the electrical length of the ith resonator at ω_0 is as given in Fig. 5.

Thus the various design equations of Fig. 5 for the waveguide direct-coupled filter have been verified. Also, Fig. 10 for the capacitive-gap-coupled transmission-line filter is seen to be verified when it is considered that λ_g in the waveguide filter formulas should be replaced by λ, and that this circuit is the dual of the waveguide circuit.

Lumped-Constant Filter Design

The resonant elements L_r, C_r in the first circuit of Fig. 3(b) are in series resonant arms. Therefore, the discussion pertaining to Fig. 11 applies, and the nversion-network characteristic impedances are given by (6). The most suitable inversion network is that of Fig. 13(d), since its negative inductance elements may be subtracted from L_r. However, this cannot be done with the first and last inversion network of the filter, since a negative inductance would be required at the input and output of the filter. This has been avoided by making $L_0 - M_{01} > 0$ and by choosing the value of M_{01} such that the proper load resistance R' (Fig. 15) will be inserted in series with the first resonant circuit. The equivalent series-inductance component M_{01}' then becomes a part of the resonant circuit, as indicated in Fig. 3(b).

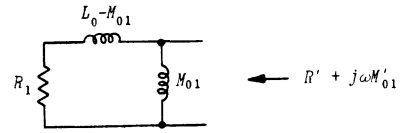

Fig. 15—Equivalent load impedance of inductive-coupled lumped-constant filter.

The capacitance-coupled lumped-constant filter of Fig. 3(a) is the dual of the circuit of Fig. 3(b) (if $L_0 = |M_{01}|$), and the formulas for one case may be obtained readily from those of the other. It will be noticed that the formulas for C_{01} and M_{01} have a somewhat different appearance, but this difference disappears when $L_0 - |M_{01}| = 0$, and the equation giving M_{01} is solved explicitly for M_{01}. However, when mutual inductance is used in a filter design, a primary inductance $L_0 > |M_{01}|$ must be provided, and the spacing to the secondary should then be adjusted to yield the necessary value of M_{01}.

The frequency-scale correction for the lumped-constant filter to allow for the frequency dependence of the inversion-network characteristic impedance is derived in the same way as for the waveguide filter. The resulting frequency relationships are given in (1), (2), and (3).

Generalized Case of Coupled Resonators—Coupling Coefficient

In the analysis of lumped-constant coupled-resonant-circuit filters, it has been customary to define a coupling coefficient k between adjacent resonant circuits. For narrow bandwidth, the coupling coefficient between resonators i and $i+1$ is related to the pass band frequencies and prototype elements by

$$k_{i,i+1} = \frac{1}{\omega_1' \sqrt{g_i g_{i+1}}} \cdot \left(\frac{f_2 - f_1}{f_0}\right).$$

This parameter is also useful in the design of narrow-band filters containing resonant cavities of any shape. The coupling element (aperture, loop, probe, etc.) to yield the desired value of coupling coefficient may be determined by calculation or by an experimental method given by Dishal [5].

BIBLIOGRAPHY

[1] Fano, R. M., and Lawson, A. W. "Microwave Filters Using Quarter-Wave Couplings," PROCEEDINGS OF THE IRE, Vol. 35 (November, 1947), pp. 1318–1323.
[2] Mumford, W. W. "Maximally Flat Filters in Waveguide," *Bell System Technical Journal*, Vol. 27 (October, 1948), pp. 648–714.
[3] Ragan, G. L. *Microwave Transmission Circuits*. New York: McGraw-Hill Book Company, Inc., 1948. Chapters 9 and 10 by R. M. Fano and A. W. Lawson.
[4] Dishal, M. "Design of Dissipative Band-Pass Filters Producing Desired Exact Amplitude-Frequency Characteristics," PROCEEDINGS OF THE IRE, Vol. 37 (September, 1949), pp. 1050–1069.
[5] Dishal, M. "Alignment and Adjustment of Synchronously Tuned Multiple-Resonant-Circuit Filters," PROCEEDINGS OF THE IRE, Vol. 39 (November, 1951), pp. 1448–1455.
[6] Dishal, M. "Two New Equations for the Design of Filters," *Electrical Communication*, Vol. 40 (December, 1953), pp. 324–337.
[7] Dishal, M. "Concerning the Minimum Number of Resonators and Minimum Unloaded-Resonator-Q Needed in Filters," *Electrical Communication*, Vol. 31 (December, 1954), pp. 257–277. Also IRE TRANSACTIONS, PGVC-3 (June, 1953), pp. 85–117.
[8] Southworth, G. C. *Principles and Applications of Waveguide Transmission*. New York: D. Van Nostrand Company, Inc., 1950, pp. 285–319.
[9] Riblet, H. J. "Synthesis of Narrow-Band Direct Coupled Filters," PROCEEDINGS OF THE IRE, Vol. 40 (October, 1952), pp. 1219–1223.
[10] Bradley, E. H., and White, D. R. "Band-Pass Filters Using Stripline Techniques," IRE TRANSACTIONS, Vol. MTT-3 (March, 1955), pp. 163–169.
[11] Bradley, E. H. "Design and Development of Strip-Line Filters," IRE TRANSACTIONS, Vol. MTT-4 (April, 1956), pp. 86–93.
[12] Belevitch, V. "Tchebyscheff Filters and Amplifier Networks," *Wireless Engineer*, Vol. 29 (April, 1952), pp. 106–110.
[13] Orchard, H. J. "Formulas for Ladder Filters," *Wireless Engineer*, Vol. 30 (January, 1953), pp. 3–5.
[14] Marcuvitz, N. *Waveguide Handbook*. (Massachusetts Institute of Technology, Radiation Laboratory Series, Vol. 10.) New York: McGraw-Hill Book Company, Inc., 1951, pp. 221, 227, 229, 238, 257, etc.
[15] Keen, H., and Sion, E. "Progress During November 1954." Contract AF 19 (604)-780, Airborne Instruments Laboratory, Mineola, N. Y. (December 1, 1954).
[16] Oliner, A. A. "Equivalent Circuits for Discontinuities in Balanced Strip Transmission Line," IRE TRANSACTIONS, Vol. MTT-3 (March, 1955), pp. 134–143.
[17] Wheeler, H. A. Wheeler Monographs, Vol. I (Wheeler Laboratories, Great Neck, L. I., N. Y.), 1953, pp. 3–54.

Distributed-Parameter Variable Delay Lines Using Skewed Turns for Delay Equalization*

F. D. LEWIS†, SENIOR MEMBER, IRE, AND R. M. FRAZIER‡, MEMBER, IRE

Summary—**Delay equalization of distributed-parameter delay lines is accomplished by a new method making use of skewed turns in the winding. A simple analysis of the basis for the use of this method of equalization is given, and the performance of experimental variable delay lines is discussed.**

A brief survey of the artificial-line delay-equalization problem is given with a discussion of some of the alternative methods of solving the problem.

INTRODUCTION

THE REALIZATION of continuously variable electromagnetic delay lines providing adequate bandwidth with constant time delay requires the adoption of certain design features which combine to make the task difficult. The requirement for continuous variation instead of step-wise adjustment means that the variable delay line is preferably made as a continuously wound distributed-parameter line with a sliding tap. In the continuous type of winding, it becomes difficult to introduce compensating network sections unless they can be put in as distributed elements. Also, single-layer constant-pitch coils wound with commonly used sizes of wire and form dimensions possess distributed constants which provide approximate self-compensation of time delay vs frequency *only* in the relatively high impedance range, or when the time delay per unit length of the line is very low. It is the purpose of this paper to describe a new method of delay equalization making use of a skewed winding to obtain a constant time delay vs frequency. This compensation method offers several important advantages, including the ability to provide delay equalization for characteristic impedances down to 150 ohms, or lower, without introducing wavelength-sensitive discontinuities. In Fig. 1, the pulse and step responses of a 1-μsec delay line using this new method of compensation are shown compared to the responses of an equivalent line without compensation. A simple analysis of the basis for using this method of compensation shows that the method is theoretically valid, and that the measured characteristics agree qualitatively with the results predicted by the analysis.

* Original manuscript received by the IRE, June 4, 1956.
† General Radio Co., Cambridge, Mass.
‡ Philco Corp., Philadelphia, Pa.

DELAY VARIATION WITH RESPECT TO FREQUENCY IN ARTIFICIAL LINES

Review of Delay Equalization Problem

Much engineering effort has been expended on the design of delay networks for various purposes. Lumped parameter pulse-forming networks are representative of specialized types of delay networks wherein the delay time is arranged to be constant at the required freque